



Fractionation and molecular characterization of natural organic matter (NOM) by solid-phase extraction followed by FT-ICR MS and ion mobility MS

Yuan Gao¹ · Wei Wang¹ · Chen He¹ · Zhi Fang¹ · Yahe Zhang¹ · Quan Shi¹

Received: 3 February 2019 / Revised: 5 May 2019 / Accepted: 24 May 2019 / Published online: 27 June 2019
© Springer-Verlag GmbH Germany, part of Springer Nature 2019

Abstract

Electrospray ionization (ESI) coupled with Fourier transform ion cyclotron resonance mass spectrometry (FT-ICR MS) has been widely used for the characterization of dissolved organic matter (DOM) extracted by solid-phase extraction (SPE) from various environmental waters. It is known that common SPE generally has a relatively low recovery and the non-polar and weakly polar components are less likely to be ionized due to ionization discrimination. However, the molecular selectivity during SPE is not clear so far. In this study, the Suwannee River natural organic matter (SRNOM) was fractionated by multi-step SPE with different solvents and the fractions were characterized by negative ESI FT-ICR MS and trapped ion mobility spectrometry-mass spectrometry (IMS-MS). The sequential solvent elution increased the extraction recovery of DOM in water by SPE and enabled the characterization of a weakly polar component, which cannot be detected in common SPE separation. The weakly polar component accounts for 5.7% in TOC for the SRNOM, which has complex but different molecular composition with methanol- and/or water-eluted fractions. Lipid-like compounds were enriched in this fraction. Compared with the polar molecules directly eluted by one-step SPE from the SRNOM, the weakly polar fractions exhibit larger molecular size. The results are helpful for understanding of the molecular composition of SRNOM, as well as other environmental waters. In addition, the study demonstrates that the combination of FT-ICR MS and IMS-MS has potential to characterize the chemical composition of a complex mixture, like DOM, to a new depth.

Keywords Dissolved organic matter · FT-ICR MS · IM-MS · Solid-phase extraction

Introduction

Dissolved organic matter (DOM) is stable organic mixture widely distributed in soil, sediment, surface water, ocean, and other environmental systems [1]. It is generally believed that DOM is formed by the process of enzymatic decomposition, oxidation, and microbial degradation of animals, plants, and microbial residues in natural environment [2, 3]. DOM is

a super-complex system which will keep challenging on chemical characterization for analytical chemistry.

In the past two decades, molecular composition of DOM was achieved with the development of high-resolution Fourier transform ion cyclotron resonance mass spectrometry (FT-ICR MS) [4–11]. It is considered that the molecular weight of DOM is normally distributing in a range of about 100–1000 Da with a central of around 400 Da [12]. The molecular composition of DOM obtained by MS analysis heavily depends on the ionization technique used [13]. Electrospray ionization (ESI) is widely used before DOM analysis because it is capable of ionizing polar compounds of the complex mixtures [4, 8]. In order to reduce the effect of ionization discrimination and to attain a full-scale understanding of the molecular composition of DOM, the application of an efficient separation is essential. Dittmar et al. [14] developed a solid-phase extraction (SPE) method to extract DOM from water by a commercial SPE product, namely PPL, which has been widely accepted for the separation of DOM from various water samples

Published in the topical collection *Close-Up of Current Developments in Ion Mobility Spectrometry* with guest editor Gérard Hopfgartner.

- ✉ Chen He
hechen@cup.edu.cn
- ✉ Quan Shi
sq@cup.edu.cn

¹ State Key Laboratory of Heavy Oil Processing, China University of Petroleum, Beijing 102249, China

because of its ease of application and appreciable carbon recovery. The method uses methanol as solvent to elute adsorbed DOM from the sorbent; however, some component could be lost in the extraction process [15, 16]. Separation selectivity of different solvents for SPE has been investigated by some researchers [17]. However, the molecular selectivity in the extraction is rarely investigated. In addition, high-resolution mass spectrometry only provides molecular composition, and structural information is unrevealed.

Ion mobility mass spectrometry (IMS), which has been developed to different types of instrument [18–20], is a modern analytical technique used to separate and identify ionized molecules in the gas phase based on their mobility in a carrier buffer gas. The mobility of an ion is related to its size, shape, mass, and charge. IMS can be used to provide information on the structural diversity of compounds, as well as the collision cross section (CCS) of the ion (molecule). Coupled with high-resolution mass spectrometry, IMS is considered as a state-of-the-art technique for the characterization of complex mixtures, such as petroleum [21–28] and DOM [29–33]. Although the resolution of mobility is unsatisfactory so far for the separation of isomers, IMS-MS should be one of the most powerful techniques for the molecular characterization of DOM.

In this paper, we characterize DOM and its fractions by using FT-ICR MS and IMS-MS. Molecular selectivity of the SPE with different elution solvents was investigated. The composition of the weak-polar fraction from a standard DOM sample was interpreted based on the MS analysis.

Experimental section

Sample preparation

Ultrapure water (H₂O) was obtained from Fisher Scientific, USA. Methanol (MeOH) and dichloromethane (DCM) of analytical grade and further distilled were used during all the experiments.

The Suwannee river natural organic matter (SRNOM) is a well-known reference material of the International Humic Substances Society (IHSS). The 2R101N SRNOM was dissolved with ultrapure water (HPLC grade) to a concentration of 50 mg/L before separation. The solution was adjusted to a pH value of 2 by 2 M HCl and then extracted by a Bond Elut PPL (500 mg, Agilent Technologies, USA) cartridge. The cartridge was firstly cleaned and conditioned using 20 mL methanol and 20 mL acidic water (pH = 2, diluted HCl solution). The SRNOM solution was loaded on the cartridge and passed through under gravity. The cartridge was then rinsed with 20 mL acidic water and dried under N₂ gas flow. For the common extraction, the cartridge was directly eluted with 10 ml MeOH to obtain the

M1 fraction. For another process, the cartridge was flushed by 10 ml H₂O/MeOH (50:50, v/v), 10 ml MeOH, and 10 ml MeOH/DCM (50:50, v/v) to obtain the fractions of WM, M, and MD, respectively.

The dissolved organic carbon (DOC) of the various fractions were analyzed by total organic carbon (TOC) analyzer (TOC-V, Shimadzu, Japan). All of the samples were dried under N₂ gas flow and redissolved in 20 mL ultrapure water for determining the DOC.

ESI FT-ICR MS

Molecular characterization was carried out on a Fourier transform ion cyclotron resonance mass spectrometry (FT-ICR MS) (Apex-Ultra, Bruker, Germany) equipped with a 9.4 Tesla superconducting magnet. The diluted SRNOM with known homologous oxygen-containing compounds was used for mass spectra calibration. The SRNOM and its fractions diluted to 50 mg/L were injected directly into electrospray ion source under negative ion mode. Ions accumulated in the hexapole and the collision cell for 0.001 s and 0.5 s, respectively, transferred into the ICR cell with a flight time of 1.0 ms. The mass spectra were acquired over 128 scans and the mass range was set to m/z 200–800.

Mass peaks with S/N higher than 6 were exported to a datasheet for further processing. Assignment of molecular formulas of DOM was performed using custom software. The generated formulas were validated by setting sensible chemical constraints (element counts: C ≤ 60, O ≤ 30, N ≤ 5, S ≤ 3; N rule; O/C ratio ≤ 2; H/C ratio ≤ 3 and mass accuracy window (set at ± 0.5 ppm)).

IMS-MS

Ion mobility MS characterization of the SRNOM and its fractions was performed by a trapped ion mobility analyzer coupled to a maXis Impact Q-TOF mass spectrometer (tims-TOF MS, Bruker Daltonics Inc.) [34–36]. Fifty milligrams per liter of DOM extracts (250 μL/h) was injected directly into electrospray ion source under negative mode. The IM separation was performed using nitrogen as a bath gas at 200 °C and the gas flow velocity was controlled at ca. 3 L/min. And the voltage of the capillary was 3.5 kV. The mass range was set at m/z 200–700 and the mass spectra were acquired over 1 min. The scan rate is 3 Hz and the 1/K0 range is set from 0.5 to 1.5. The ion accumulation time and ramp time were 10 ms and 300 ms. The deflector transfer to capillary exit (V_{def}), funnel 1 to deflection discard (V_{fun}), and ramp start to accumulation exit (V_{ramp}) voltages were set at $V_{\text{def}} = 150$ V, $V_{\text{fun}} = 300$ V, $V_{\text{ramp}} = -100$ V.

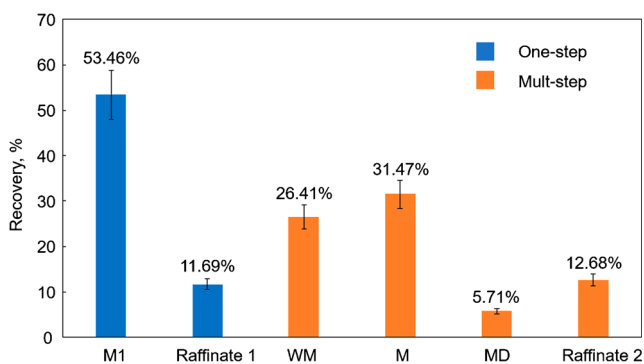


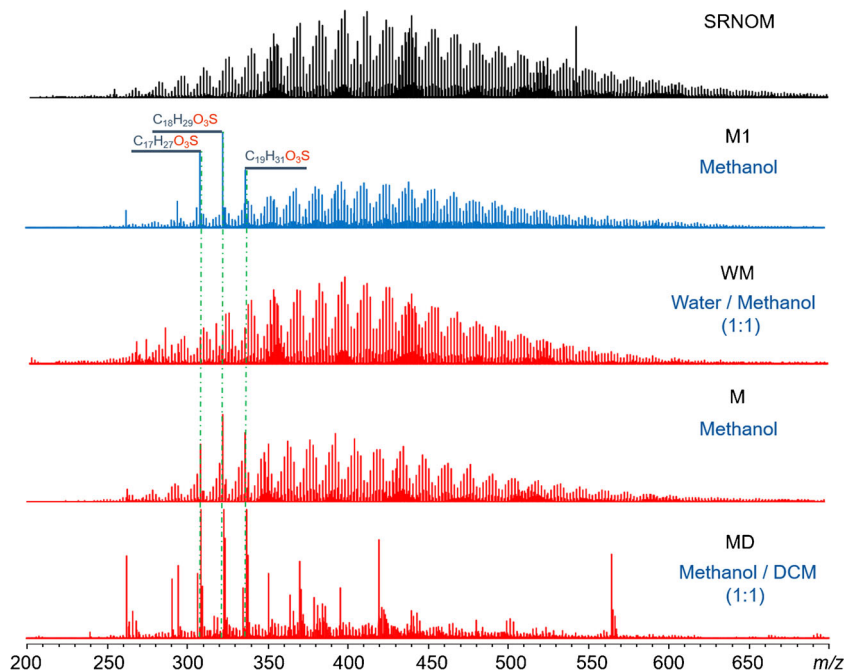
Fig. 1 DOC recovery of the extraction fractions and raffinates

Results and discussion

Total organic carbon analysis

The extraction efficiency of the multi-step SPE for DOM was evaluated in DOC value. Figure 1 shows the DOC recoveries of the various fractions. The recoveries of hydrophilic components of WM and M are 26.4% and 31.5%, respectively. The recovery of the hydrophobic component of MD is 5.71%. The recovery of one-step extraction M1 is 53.46%. The recoveries of one-step and multi-step raffinates are 11.69% and 12.68%, respectively. The total DOC of each fraction eluted by the multi-step extraction is up to 63.59%, which is significantly improved comparing with one-step extraction. The cumulative results suggest that the multi-step extraction is a better method of preliminary treatment for SRNOM (The data are averages of three experiments.). A total of 24.7% loss in TOC in the multi-step extraction may be

Fig. 2 Broadband-ESI FT-ICR mass spectra of SRNOM and its fractions (M1, WM, M, and MD)



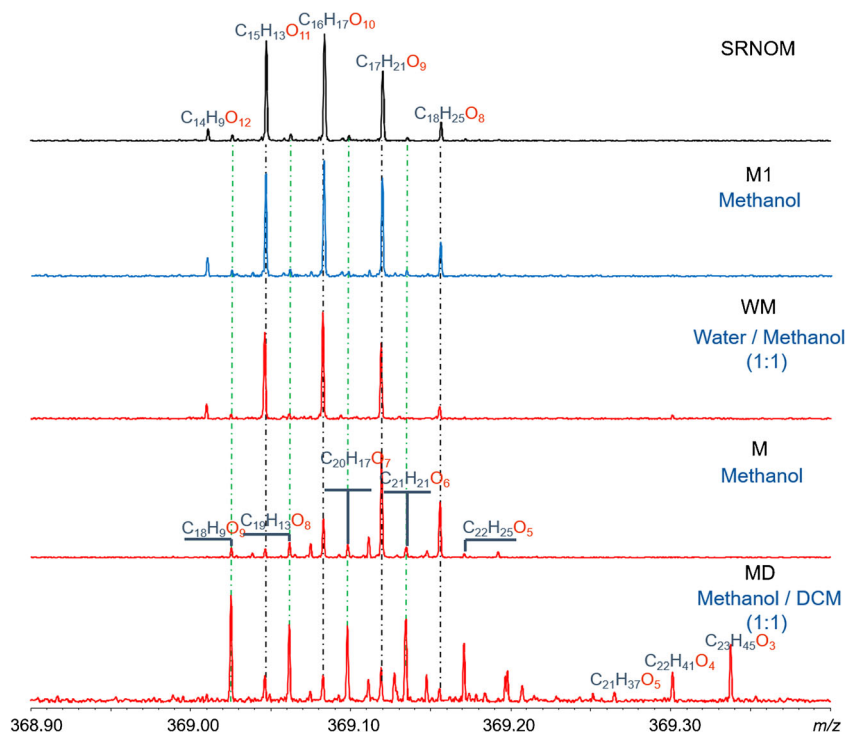
caused by the following reasons: (1) the part of DOM remained on the PPL column and was not completely eluted and (2) N_2 gas flow was used to remove the solvent during experiments, which would cause a certain loss. In the multi-step extraction, DOCs of WM and M are high, because the SRNOM contains more polar components which are easily retained in water and methanol. It should be noted that the recoveries in this experiment are lower than those reported previously [37, 38]; this is mainly caused by excessive N_2 gas flows to remove the organic solvents before TOC measurement.

Regardless of the total recovery, results shown in Fig. 1 indicate that about 12% TOC is not retained by the SPE cartridge. Total TOC of W/M and M (57.88%) in the multi-step SPE shows a little higher than that of the methanol one-step SPE (53.46%), this little difference in TOC could be caused by the operation, and we do not tend to give more interpretation on it due to the poor mass balance in the experiment. However, it is confirmed that the total yield of WM and M of the multi-step SPE must not less than M1. In other words, the fraction of MD is the component that adsorbed in the cartridge and cannot be eluted out by water and methanol. These compounds were not being characterized in most previous studies.

Molecular composition of different SPE fractions

Figure 2 shows the negative-ion-ESI FT-ICR MS spectra of the SRNOM and its fractions. The mass spectra of SRNOM, M1, WM, and M exhibit normal distributions. The range of molecular weight distribution is mainly in 250–700 Da. The

Fig. 3 Mass scale-expanded segments (m/z 369) of negative-ion FT-ICR mass spectra of SRNOM and its fractions

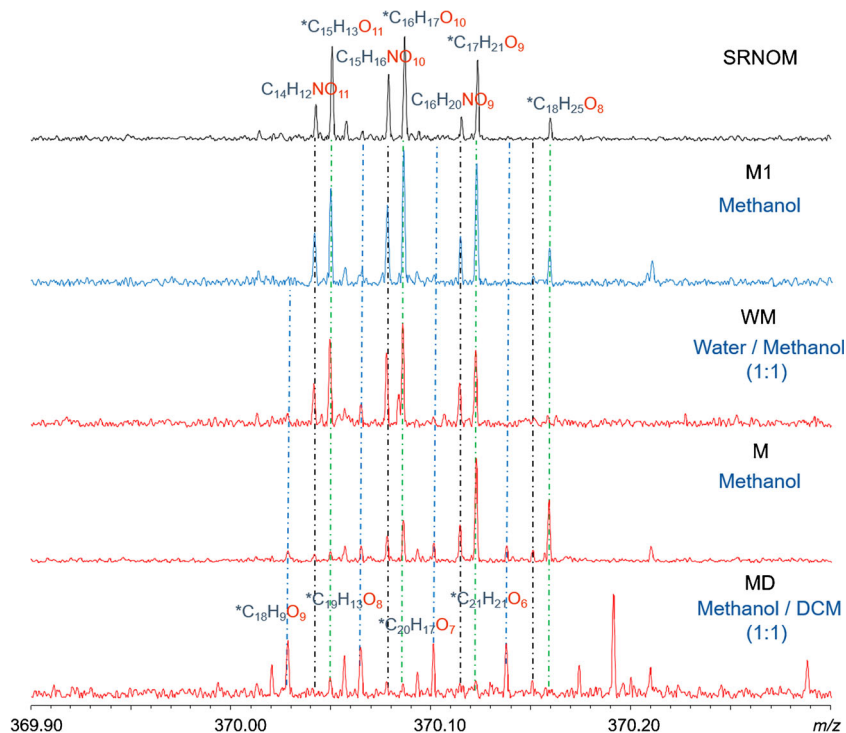


weakly polar fraction, MD exhibits an overall lower peaks intensity (values are not shown) than other fractions, which should be due to the low ionization efficiency in negative-ion ESI. The peaks of 311, 325, and 339 appearing in M1, M, and MD are identified as O_3S_1 compounds with a DBE value of 4 corresponding to alkylbenzene sulfonates, which are

considered as contaminants of anthropogenic activity and widely present in various water systems.

Figure 3 shows mass scale-expanded segments (m/z 369) of the negative-ion ESI FT-ICR mass spectra of SRNOM and its fractions. Molecular composition of each peak was assigned based on accurate mass value. Detected compounds in

Fig. 4 Mass scale-expanded segments (m/z 370) of negative-ion FT-ICR mass spectra of SRNOM and its fractions



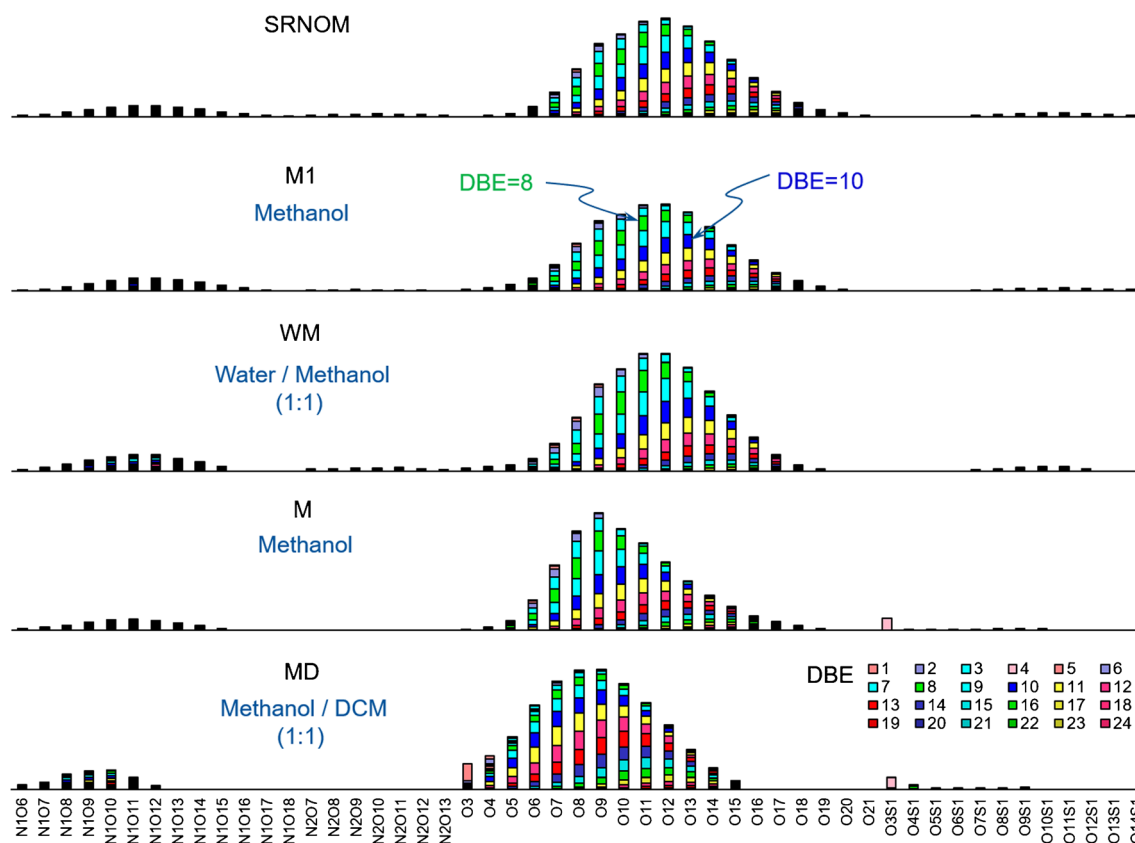


Fig. 5 Relative abundance of class species assigned from the mass spectra of SRNOM and its fractions

SRNOM, M1, and WM are a series of CHO compounds with oxygen numbers from 8 to 12 and DBE values from 6 to 10. In addition, a series of low-intensity peaks with lower oxygen numbers from 5 to 9 and higher DBE values from 10 to 14 were also detected. The relative abundance of these compounds increase in M and MD fractions indicates that they are hydrophobic CHO compounds. The intensity of the hydrophobic compounds is higher than that of the hydrophilic oxygen-containing compounds in MD, indicating that the hydrophobic compounds are enriched in methanol and DCM fraction (M and MD). It should be noted that compounds with very low DBE values such as $C_{21}H_{37}O_5$, $C_{22}H_{41}O_4$, and $C_{23}H_{45}O_3$ which were not

detected in SRNOM and M1 were also detected in MD. The result illustrates that a multi-step elution enables the enrichment and detection of these weak-polar component.

Figure 4 shows the expanded spectra at m/z 370, in which nitrogen containing compounds can be observed. Nitrogen-containing compounds exhibit a very low relative abundance, most of them are in the polar fractions (M1 and WM). Abundant peaks are ^{13}C isotope ions of CHO compounds corresponding to mass peaks of m/z 369.

Assigned compounds were classified into several class species and their relative abundance were shown in Fig. 5. Compound classes include N_1O_x , N_2O_x , O_x , and O_xS_1 , of which O_x compounds are dominant. Class species are N_1O_{6-18} , N_2O_{7-13} , O_{4-21} , and $O_{7-14}S_1$ for SRNOM; N_1O_{6-17} , N_2O_{7-12} , O_{3-20} , and $O_{7-14}S_1$ for M1; N_1O_{6-15} , N_2O_{7-13} , O_{3-19} , and $O_{7-12}S_1$ for WM; N_1O_{6-15} , O_{3-19} , and $O_{3-10}S_1$ for M; N_1O_{6-12} , O_{3-15} , and $O_{3-9}S_1$ for MD. With the decrease of solvent polarity, the upper limits of the oxygen number gradually decrease and the most abundant class species shifts to a lower value (from 12 in WM to 8 in MD). This is consistent with the finding in previous studies which using sequential elution SPE [39–41]. The N_2O_x compounds are enriched in the WM and not detected in M and MD, indicating that these nitrogen-containing compounds have strong molecular polarity.

Amount of molecule assigned from the spectra of the DOM and its fractions are listed in Table 1. More molecules were

Table 1 The number of molecular formulas assigned from the FT-ICR mass spectra of SRNOM and its SPE fractions

Class species	Non-SPE SRNOM	One-step SPE M1	Multi-step SPE			Total*
			WM	M	MD	
O_x	2239	2279	1340	2240	1758	3028
N_1O_x	769	804	505	829	468	1057
N_2O_x	171	62	101	0	0	101
O_xS_1	237	175	115	114	50	250
Total	3416	3320	2061	3183	2276	4436

*Duplicates have been removed

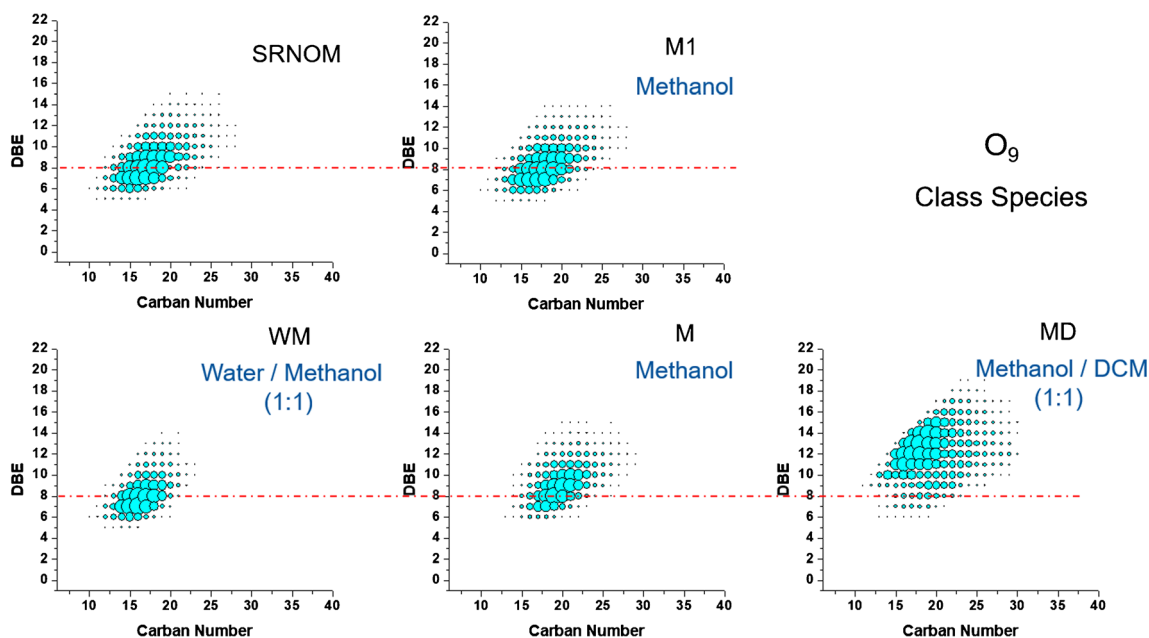


Fig. 6 Ion relative abundance plots of DBE versus carbon number for O_9 class species in SRNOM and its fractions

detected for the multi-step SPE except N_2O_x class species. The total assigned molecules of the multi-step SPE is 4436, which is much higher than that from the one-step SPE (3320).

To investigate the compositional difference in SRNOM and its fractions, ion relative abundance plots of DBE versus carbon number for the O_9 class species, as an example, were plotted in Fig. 6. The size of the dot in the figure is related to the ion relative abundance. The DBE value and carbon number of SRNOM, M1, WM, and M are in a relatively narrow range, with values of 10–25 and 4–14, respectively. While for

MD, the carbon number and the DBE value ranges both shift to higher values (C_{10} – C_{30} with $DBE = 6$ – 18). The result indicates that the structures of compounds in MD (hydrophobic) are largely different from that in other fractions (hydrophilic). The high DBE values imply that the hydrophobic compound has more condensed aromatic ring structures.

The van Krevelen diagrams of various fractions are shown in Fig. 7, which showed the distribution of assigned molecules in hydrogen to carbon (H/C) and oxygen to carbon (O/C) ratios. Compounds in SRNOM, M1,

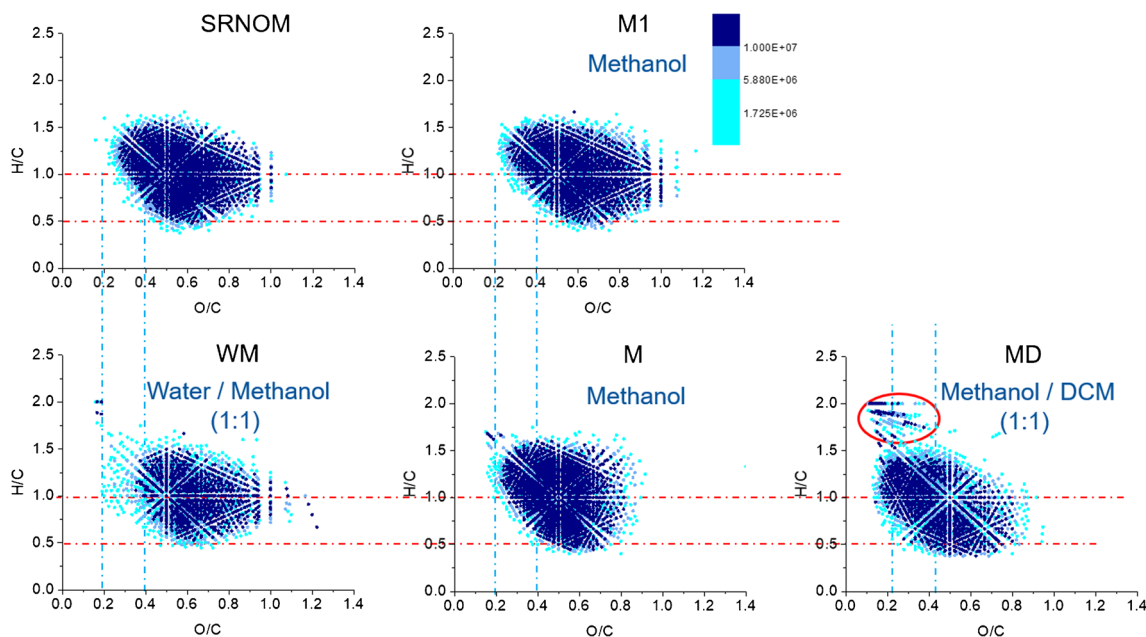


Fig. 7 Van Krevelen diagram of SRNOM and its SPE fractions

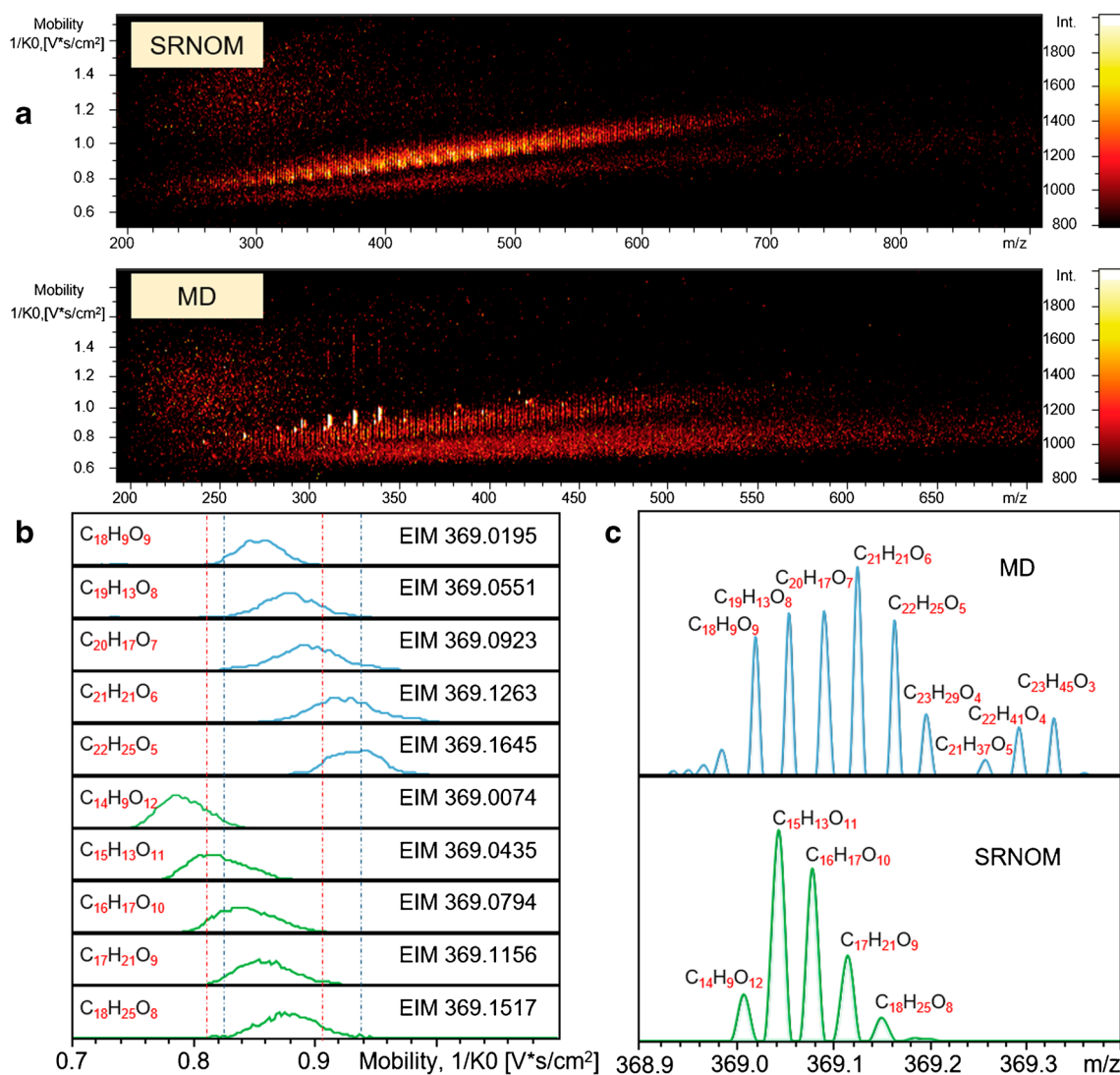


Fig. 8 **a** IM-MS spectra of SRNOM and MD. **b** Extracted ion mobility spectra of m/z 369.0195, 369.0551, 369.0923, 369.1263, and 369.1645 for MD and m/z 369.0074, 369.0435, 369.0794, 369.1156, and 369.1517 for SRNOM. **c** Mass scale-expanded mass spectra of MD and SRNOM obtained from the tims-TOF MS at m/z 369

for SRNOM. **c** Mass scale-expanded mass spectra of MD and SRNOM obtained from the tims-TOF MS at m/z 369

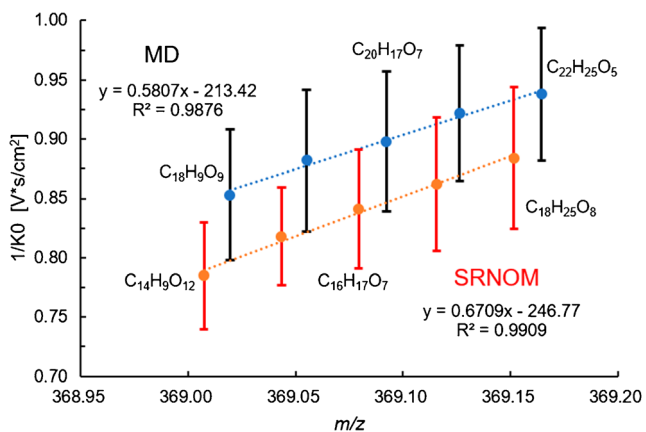


Fig. 9 $1/KO$ as a function of m/z for oxygen-containing compounds in the SRNOM and MD fraction at m/z 369

and WM mainly located in a region of $O/C = 0.2$ – 1.0 and $H/C = 0.5$ – 1.5 ; compounds in M are mainly located in a region of $O/C = 0.2$ – 0.8 , $H/C = 0.5$ – 1.7 ; compounds in MD are mainly located in a region of $O/C = 0.2$ – 0.8 , $H/C = 0.4$ – 2.0 . With the decreasing of solvent polarity, the eluted compounds shift toward lower O/C and higher H/C region. Polar compounds of O/C more than 0.8 are mainly enriched in WM, which correspond to tannins and are strongly hydrophilic compounds [42–44]. Hydrophobic compounds eluted in MD are mainly in the region of $O/C = 0.2$ – 0.4 and $H/C = 0.5$ – 1.0 , corresponding to condensed aromatics. Compounds presented in the top-left corner of MD with high H/C and low O/C ($O/C = 0$ – 0.3 , $H/C = 1.5$ – 2), which generally classified into lipids, are cannot be detected without the separation. These compounds corresponding the peaks close the right end of the

MD mass spectrum in Fig. 3. The molecules of $C_{23}H_{45}O_3$, $C_{22}H_{41}O_4$, and $C_{21}H_{37}O_5$ are more likely 1–3 naphthenic ring alcohols.

Ion mobility characterization of SRNOM and its fraction

Figure 8 shows the IMS-MS results of the SRNOM and MD fraction. We just select a narrow mass range, m/z 369, which has been analyzed by FT-ICR MS as shown in Fig. 3 for the illustration. TOF MS generally is incompetent in mass resolution for DOM analysis, comparing with Fig. 3; however, the mass peaks in Fig. 8c of SRNOM can be considered as a complete separation of different molecular composition. Most peaks of MD are also with exclusive molecular composition.

The abscissa axis of mobility spectra shown in Fig. 8b uses a unit of $1/K_0$, which can be replaced by CCS (collision cross section) value. For the convenience of discussion, we generally use CCS in the following text. As shown in Fig. 8b, mobiligram (ion mobility chromatogram) peak of each selected ion exhibits a nearly normal distribution and expands a large CCS value range (around 0.12 units), which is about 2 times in peak width to an individual compound (around 0.06 units). This is an evidence for the speculation based on chromatographic analysis that the DOM molecule has enormous isomers.

Figure 9 shows $1/K_0$ as a function of m/z for mass peaks of the SRNOM and MD fraction at m/z 369. The $1/K_0$ and m/z exhibit good linear relationship with equations of $y = 0.5807x - 213.42$ ($R = 0.9876$) and $y = 0.6709x - 246.77$ ($R = 0.9909$) for MD and SRNOM, respectively. Two adjacent points in each line have difference in molecular composition of an O vs CH_4 . With the increasing of degree of oxidation, one CH_4 replaced with an oxygen atom, CCS value of the compounds decrease; in other words, the molecule is more compact.

The equations of SRNOM and MD show different intercepts and slopes, which means that hydrophobic oxygenates and hydrophilic oxygenates have different stem-nucleus structures. For O_9 class species, for example, when 12 hydrogen atoms in the molecule are replaced by one carbon atom, the accurate molecular weight changed obviously in high-resolution mass spectrum but the change in CCS value is hardly observed. For isobaric molecules, the oxidation degree has higher influence than condensation degree of hydrocarbon skeleton of the molecule on its CCS value. As shown in Figs. 8 and 9, hydrophobic compounds as a whole have larger CCS value than those of hydrophilic isobaric molecules. IMS-MS can be considered as a two-dimensional mass spectrometry; however, most commercial instruments are based on TOF MS, which cannot provide enough mass resolving power to obtain a real two-dimensional analysis for complex mixture:

the mobiligram of a given mass value generally containing different molecular compositions. IMS coupled with FT-ICR MS is capable for an IMS analysis of an exclusive molecule, but the interpretation of CCS profile is rarely discussed because the structures of the DOM and/or petroleum molecules are unclear. The finding of this work is instructive for the interpretation of IMS-MS spectra as well as the understanding of the structural composition of the natural complex mixtures.

Conclusion

The sequential solvent elution increased the extraction recovery of DOM in water by SPE and enabled the characterization of weak-polar component, which cannot be detected in the common SPE separation. The weak-polar component account for a 5.7% in TOC for the SRNOM, which has complex but different molecular composition with methanol and/or water eluted fractions. Lipid-like compounds were enriched in this fraction. Compared with the polar molecules directly eluted by one-step SPE from the SRNOM, the weak-polar fractions exhibit larger molecular size. The results are helpful for the understanding of the molecular composition of SRNOM, as well as other environmental waters. In addition, the study demonstrates that the combination of FT-ICR MS and IMS-MS is potential to characterize the chemical composition of complex mixture, like DOM to a new depth.

Funding information This work was supported by the National Key Research and Development Program of China (2018YFA0605800).

Compliance with ethical standards

Compliance with ethical standards The authors declare that they have no conflicts of interest.

References

1. Leenheer JA, Nanny MA, McIntyre C. Terpenoids as major precursors of dissolved organic matter in landfill leachates, surface water, and groundwater. *Environ Sci Technol.* 2003;37(11):2323–31. <https://doi.org/10.1021/es0264089>.
2. Kristensen E, Bouillon S, Dittmar T, Marchand C. Organic carbon dynamics in mangrove ecosystems: a review. *Aquat Bot.* 2008;89(2):201–19. <https://doi.org/10.1016/j.aquabot.2007.12.005>.
3. Ward ND, Keil RG, Medeiros PM, Brito DC, Cunha AC, Dittmar T, et al. Degradation of terrestrially derived macromolecules in the Amazon River. *Nat Geosci.* 2013;6(7):530–3. <https://doi.org/10.1038/ngeo1817>.
4. Fievre A, Solouki T, Marshall AG, Cooper WT. High-resolution Fourier transform ion cyclotron resonance mass spectrometry of humic and fulvic acids by laser desorption/ionization and electrospray ionization. *Energy Fuel.* 1997;11(3):554–60. <https://doi.org/10.1021/ef970005q>.

5. Kujawinski EB, Del Vecchio R, Blough NV, Klein GC, Marshall AG. Probing molecular-level transformations of dissolved organic matter: insights on photochemical degradation and protozoan modification of DOM from electrospray ionization Fourier transform ion cyclotron resonance mass spectrometry. *Mar Chem.* 2004;92(1–4):23–37. <https://doi.org/10.1016/j.marchem.2004.06.038>.
6. Sleighter RL, Mckee GA, Liu Z, Hatcher PG. Naturally present fatty acids as internal calibrants for Fourier transform mass spectra of dissolved organic matter. *Limnol Oceanogr Methods.* 2008;6(2):246–53. <https://doi.org/10.4319/lom.2008.6.246>.
7. Herzprung P, Hertkorn N, von Tuempling W, Harir M, Friese K, Schmitt-Kopplin P. Molecular formula assignment for dissolved organic matter (DOM) using high-field FT-ICR-MS: chemical perspective and validation of sulphur-rich organic components (CHOS) in pit lake samples. *Anal Bioanal Chem.* 2016;408(10):2461–9. <https://doi.org/10.1007/s00216-016-9341-2>.
8. Koch BP, Witt MR, Engbrodt R, Dittmar T, Kattner G. Molecular formulae of marine and terrigenous dissolved organic matter detected by electrospray ionization Fourier transform ion cyclotron resonance mass spectrometry. *Geochim Cosmochim Acta.* 2005;69(13):3299–308. <https://doi.org/10.1016/j.gca.2005.02.027>.
9. Gonsior M, Peake BM, Cooper WT, Podgorski D, D'Andrilli J, Cooper WJ. Photochemically induced changes in dissolved organic matter identified by ultrahigh resolution Fourier transform ion cyclotron resonance mass spectrometry. *Environ Sci Technol.* 2009;43(3):698–703. <https://doi.org/10.1021/es8022804>.
10. Mangal V, Stock NL, Gueguen C. Molecular characterization of phytoplankton dissolved organic matter (DOM) and sulfur components using high resolution Orbitrap mass spectrometry. *Anal Bioanal Chem.* 2016;408(7):1891–900. <https://doi.org/10.1007/s00216-015-9295-9>.
11. Nebbioso A, Piccolo A. Molecular characterization of dissolved organic matter (DOM): a critical review. *Anal Bioanal Chem.* 2013;405(1):109–24. <https://doi.org/10.1007/s00216-012-6363-2>.
12. He C, Jiang B, Shi Q, Hsu CS. Comment on “laser desorption/ionization coupled to FTICR mass spectrometry for studies of natural organic matter”. *Anal Chem.* 2018;90(9):5965–7. <https://doi.org/10.1021/acs.analchem.8b00332>.
13. Ohno T, Sleighter RL, Hatcher PG. Comparative study of organic matter chemical characterization using negative and positive mode electrospray ionization ultrahigh-resolution mass spectrometry. *Anal Bioanal Chem.* 2016;408(10):2497–504. <https://doi.org/10.1007/s00216-016-9346-x>.
14. Dittmar T, Koch B, Hertkorn N, Kattner G. A simple and efficient method for the solid-phase extraction of dissolved organic matter (SPE-DOM) from seawater. *Limnol Oceanogr Methods.* 2008;6(6):230–5.
15. Chen M, Kim S, Park J-E, Kim HS, Hur J. Effects of dissolved organic matter (DOM) sources and nature of solid extraction sorbent on recoverable DOM composition: implication into potential lability of different compound groups. *Anal Bioanal Chem.* 2016;408(17):4809–19. <https://doi.org/10.1007/s00216-016-9569-x>.
16. Chen M, Kim S, Park J-E, Jung H-J, Hur J. Structural and compositional changes of dissolved organic matter upon solid-phase extraction tracked by multiple analytical tools. *Anal Bioanal Chem.* 2016;408(23):6249–58. <https://doi.org/10.1007/s00216-016-9728-0>.
17. Lewis AT, Tekavec TN, Jarvis JM, Juyal P, McKenna AM, Yen AT, et al. Evaluation of the extraction method and characterization of water-soluble organics from produced water by Fourier transform ion cyclotron resonance mass spectrometry. *Energy Fuel.* 2013;27(4):1846–55. <https://doi.org/10.1021/ef3018805>.
18. Ridgeway ME, Lubeck M, Jordens J, Mann M, Park MA. Trapped ion mobility spectrometry: a short review. *Int J Mass Spectrom.* 2018;425:22–35.
19. Cumeras R, Figueras E, Davis CE, Baumbach JI, Gràcia I. Review on ion mobility spectrometry. Part 1: current instrumentation. *Analyst.* 2015;140(5):1376. <https://doi.org/10.1039/c4an01100g>.
20. May JC, Mclean JA. Ion mobility-mass spectrometry: time-dispersive instrumentation. *Anal Chem.* 2015;87(3):1422–36. <https://doi.org/10.1021/ac504720m>.
21. Huang R, McPhedran KN, Gamal El-Din M. Ultra performance liquid chromatography ion mobility time-of-flight mass spectrometry characterization of naphthenic acids species from oil sands process-affected water. *Environ Sci Technol.* 2015;49(19):11737–45. <https://doi.org/10.1021/acs.est.5b03178>.
22. Noestheden MR, Headley JV, Peru KM, Barrow MP, Burton LL, Sakuma T, et al. Rapid characterization of naphthenic acids using differential mobility spectrometry and mass spectrometry. *Environ Sci Technol.* 2014;48(17):10264–72. <https://doi.org/10.1021/es501821h>.
23. Lalli PM, Jarvis JM, Marshall AG, Rodgers RP. Functional isomers in petroleum emulsion interfacial material revealed by ion mobility mass spectrometry and collision-induced dissociation. *Energy Fuel.* 2017;31(1):311–8. <https://doi.org/10.1021/acs.energyfuels.6b02411>.
24. Lalli PM, Corilo YE, Rowland SM, Marshall AG, Rodgers RP. Isomeric separation and structural characterization of acids in petroleum by ion mobility mass spectrometry. *Energy Fuel.* 2015;29(6):150516102226003.
25. Arif A, Yunju C, Kevin G, Eleanor R, Jong Wha L, Kim HL, et al. Elucidating molecular structures of nonalkylated and short-chain alkyl ($n < 5$, $(CH_2)_n$) aromatic compounds in crude oils by a combination of ion mobility and ultrahigh-resolution mass spectrometry and theoretical collisional cross-section calculations. *Anal Chem.* 2014;86(7):3300.
26. Fernandez-Lima FA, Christopher B, McKenna AM, Rodgers RP, Marshall AG, Russell DH. Petroleum crude oil characterization by IMS-MS and FTICR MS. *Anal Chem.* 2009;81(24):9941–7.
27. Becker C, Qian K, Russell DH. Molecular weight distributions of asphaltenes and deasphalted oils studied by laser desorption ionization and ion mobility mass spectrometry. *Anal Chem.* 2008;80(22):8592–7.
28. Benigni P, Fernandez-Lima F. Oversampling selective accumulation trapped ion mobility spectrometry coupled to FT-ICR MS: fundamentals and applications. *Anal Chem.* 2016;88(14):acs.analchem.6b01946.
29. Benigni P, Thompson CJ, Ridgeway ME, Park MA, Fernandez-Lima F. Targeted high-resolution ion mobility separation coupled to ultrahigh-resolution mass spectrometry of endocrine disruptors in complex mixtures. *Anal Chem.* 2015;87(8):4321–5. <https://doi.org/10.1021/ac504866v>.
30. Tose LV, Benigni P, Leyva D, Sundberg A, Ramírez CE, Ridgeway ME, et al. Coupling trapped ion mobility spectrometry to mass spectrometry: TIMS-TOF MS vs TIMS-FT-ICR MS. *Rapid Commun Mass Spectrom.* 2018;32(15):1287–1295. <https://doi.org/10.1002/rcm.8165>.
31. Lu K, Gardner WS, Liu Z. Molecular structure characterization of riverine and coastal dissolved organic matter with ion mobility quadrupole time-of-flight LCMS (IM Q-TOF LCMS). *Environ Sci Technol.* 2018;52(13):7182–91.
32. Benigni P, Sandoval K, Thompson CJ, Ridgeway ME, Park MA, Gardinali P, et al. Analysis of photoirradiated water accommodated fractions of crude oils using tandem TIMS and FT-ICR MS. *Environ Sci Technol.* 2017;51(11):5978.
33. Benigni P, Marin R, Sandoval K, Gardinali P, Fernandez-Lima F. Chemical analysis of water-accommodated fractions of crude oil

- spills using TIMS-FT-ICR MS. *J Vis Exp Jove*. 2017;2017(121):55352. <https://doi.org/10.3791/55352>.
34. Hernandez DR, Debord JD, Ridgeway ME, Kaplan DA, Park MA, Fernandezlima F. Ion dynamics in a trapped ion mobility spectrometer. *Analyst*. 2014;139(8):1913–21.
 35. Fernandezlima FA, Kaplan DA, Park MA. Note: integration of trapped ion mobility spectrometry with mass spectrometry. *Rev Sci Instrum*. 2011;82(12):93.
 36. Fernandezlima F, Kaplan DA, Suetering J, Park MA. Gas-phase separation using a trapped ion mobility spectrometer. *Int J Ion Mobil Spectrom*. 2011;14(2–3):93–8.
 37. Li Y, Harir M, Lucio M, Kanawati B, Smirnov K, Flerus R, et al. Proposed guidelines for solid phase extraction of Suwannee River dissolved organic matter. *Anal Chem*. 2016;88(13):6680–8. <https://doi.org/10.1021/acs.analchem.5b04501>.
 38. Li Y, Harir M, Uhl J, Kanawati B, Lucio M, Smirnov KS, et al. How representative are dissolved organic matter (DOM) extracts? A comprehensive study of sorbent selectivity for DOM isolation. *Water Res*. 2017;116(3):316–23. <https://doi.org/10.1016/j.watres.2017.03.038>.
 39. Liu Z, Sleighter RL, Zhong J, Hatcher PG. The chemical changes of DOM from black waters to coastal marine waters by HPLC combined with ultrahigh resolution mass spectrometry. *Estuar Coast Shelf Sci*. 2011;92(2):205–16. <https://doi.org/10.1016/j.ecss.2010.12.030>.
 40. Repeta DJ. Chapter 2 – Chemical characterization and cycling of dissolved organic matter. In: *Biogeochemistry of Marine Dissolved Organic Matter*; 2015. p. 21–63. <https://doi.org/10.1016/B978-0-12-405940-5.00002-9>.
 41. Lu K, Gardner WS, Liu Z. Molecular structure characterization of riverine and coastal dissolved organic matter with ion mobility quadrupole time of flight LCMS (IM Q-TOF LCMS). *Environ Sci Technol*. 2018. <https://doi.org/10.1021/acs.est.8b00999>.
 42. Herzsprung P, von Tuempling W, Hertkom N, Harir M, Buettner O, Bravidor J, et al. Variations of DOM quality in inflows of a drinking water reservoir: linking of van Krevelen diagrams with EEMF spectra by rank correlation. *Environ Sci Technol*. 2012;46(10):5511–8. <https://doi.org/10.1021/es300345c>.
 43. Kim S, Kramer RW, Hatcher PG. Graphical method for analysis of ultrahigh-resolution broadband mass spectra of natural organic matter, the van Krevelen diagram. *Anal Chem*. 2003;75(20):5336–44. <https://doi.org/10.1021/ac034415p>.
 44. Sleighter RL, Hatcher PG. Molecular characterization of dissolved organic matter (DOM) along a river to ocean transect of the lower Chesapeake Bay by ultrahigh resolution electrospray ionization Fourier transform ion cyclotron resonance mass spectrometry. *Mar Chem*. 2008;110(3):140–52.

Publisher's note Springer Nature remains neutral with regard to jurisdictional claims in published maps and institutional affiliations.